Journal of Statistical Mechanics:
Theory and Experiment

SISSA

PAPER: CLASSICAL STATISTICAL MECHANICS, EQUILIBRIUM AND NON-EQUILIBRIUM

Statistics of first-passage Brownian functionals

Journal of Statistical Mechanics: Theory and Experiment
An IOP and SISSA journal

PAPER: Classical statistical mechanics, equilibrium and non-equilibrium

Statistics of first-passage Brownian functionals

Satya N Majumdar[1] **and Baruch Meerson**[2]

[1] LPTMS, CNRS, Univ. Paris-Sud, Université Paris-Saclay, 91405 Orsay, France
[2] Racah Institute of Physics, Hebrew University of Jerusalem, Jerusalem 91904, Israel
E-mail: satya.majumdar@u-psud.fr and meerson@mail.huji.ac.il

Received 15 November 2019
Accepted for publication 2 December 2019
Published 11 February 2020

Online at stacks.iop.org/JSTAT/2020/023202
https://doi.org/10.1088/1742-5468/ab6844

Abstract. We study the distribution of first-passage functionals of the type $\mathcal{A} = \int_0^{t_f} x^n(t)\,\mathrm{d}t$ where $x(t)$ represents a Brownian motion (with or without drift) with diffusion constant D, starting at $x_0 > 0$, and t_f is the first-passage time to the origin. In the driftless case, we compute exactly, for all $n > -2$, the probability density $P_n(A|x_0) = \mathrm{Prob.}(\mathcal{A} = A)$. We show that $P_n(A|x_0)$ has an essential singular tail as $A \to 0$ and a power-law tail $\sim A^{-(n+3)/(n+2)}$ as $A \to \infty$. The leading essential singular behavior for small A can be obtained using the optimal fluctuation method (OFM), which also predicts the optimal paths of the conditioned process in this limit. For the case with a drift toward the origin, where no exact solution is known for general $n > -1$, we show that the OFM successfully predicts the tails of the distribution. For $A \to 0$ it predicts the same essential singular tail as in the driftless case. For $A \to \infty$ it predicts a stretched exponential tail $-\ln P_n(A|x_0) \sim A^{1/(n+1)}$ for all $n > 0$. In the limit of large Péclet number $\mathrm{Pe} = \mu x_0/(2D)$, where μ is the drift velocity toward the origin, the OFM predicts an exact large-deviation scaling behavior, valid for all A: $-\ln P_n(A|x_0) \simeq \mathrm{Pe}\,\Phi_n\left(z = A/\bar{A}\right)$, where $\bar{A} = x_0^{n+1}/\mu(n+1)$ is the mean value of $\mathcal{A}$ in this limit. We compute the rate function $\Phi_n(z)$ analytically for all $n > -1$. We show that, while for $n > 0$ the rate function $\Phi_n(z)$ is analytic for all z, it has a non-analytic behavior at $z = 1$ for $-1 < n < 0$ which can be interpreted as a dynamical phase transition. The order of this transition is 2 for $-1/2 < n < 0$, while for $-1 < n < -1/2$ the order of transition is $1/(n+1)$; it changes continuously with n. We also provide an illuminating alternative derivation of the OFM result by using a WKB-type asymptotic perturbation

theory for large Pe. Finally, we employ the OFM to study the case of $\mu < 0$ (drift away from the origin). We show that, when the process is conditioned on reaching the origin, the distribution of $\mathcal{A}$ coincides with the distribution of $\mathcal{A}$ for $\mu > 0$ with the same $|\mu|$.

Keywords: Brownian motion, large deviations in non-equilibrium systems, classical phase transitions, fluctuation phenomena

Contents

1. Introduction

Functionals of Brownian motion appear naturally in many different contexts spanning across physics, chemistry, biology, computer science and mathematics (see [1] for a review). Statistical properties of the functionals of a one-dimensional Brownian motion over a fixed time interval have been studied extensively since the celebrated

Feynman–Kac formula [2]. Another class of functionals of one-dimensional Brownian motion have also attracted quite a lot of attention, namely the *first-passage* Brownian functional, defined up to the time of first passage of the Brownian motion, starting say at $x_0 > 0$, to a certain point in space, e.g. the origin [1]. More precisely, let us consider a one-dimensional Brownian motion $x(t)$ with diffusion constant D that starts at $x_0 > 0$ and evolves in time via the Langevin equation

$$\frac{\mathrm{d}x}{\mathrm{d}t} = \eta(t)\,, \tag{1}$$

where $\eta(t)$ is the Gaussian white noise with zero mean and the correlator $\langle \eta(t)\eta(t')\rangle = 2\,D\,\delta(t-t')$. Let t_f denote the first time the process $x(t)$ crosses the origin. Clearly t_f is a random variable that varies from trajectory to trajectory. Let us define a random functional

$$\mathcal{A} = \int_0^{t_f} U(x(t))\,\mathrm{d}t, \tag{2}$$

where $U(x)$ can, in principle, be an arbitrary function. One is interested in computing the probability distribution $P(A|x_0)$ that the functional $\mathcal{A}$ takes a specified value A, given the starting position of the particle x_0. Motivated by several physical examples (see below), we will focus here on scale-free functionals, where $U(x) = x^n$, with $n > -2$ as we justify later. Thus our object of interest is the probability density function (PDF) $P_n(A|x_0)$ that the first-passage functional

$$\mathcal{A} = \int_0^{t_f} [x(t)]^n\,\mathrm{d}t \tag{3}$$

takes the value A. There are many examples where this family of functionals is of relevance. For example, $n = 0$ corresponds to $\mathcal{A} = t_f$, that is the first-passage time itself, whose exact distribution is well known [3, 4]:

$$P_0(t_f|x_0) = \frac{x_0}{\sqrt{4\,\pi\,D}}\,t_f^{-3/2}\,\exp\left(-\frac{x_0^2}{4\,D\,t_f}\right)\,. \tag{4}$$

For large $t_f \gg x_0^2$, the PDF $P_0(t_f|x_0)$ has a power-law tail, $P_0(t_f|x_0) \sim t_f^{-3/2}$. In contrast, at $t_f \to 0$, the PDF has an essential singularity $P_0(t_f|x_0) \sim \exp\left(-\frac{x_0^2}{4\,D\,t_f}\right)$. Another example concerns the case $n = 1$, where $\mathcal{A} = \int_0^{t_f} x(t)\mathrm{d}t$ is the area swept by the Brownian motion till its first-passage time, and its distribution was computed exactly in [5]. This particular case $n = 1$ has many applications ranging from queueing theory and combinatorics, all the way up to the statistics of avalanches in self-organized criticality [5]. For example, in the context of the queueing theory, $x(t)$ may represent the length of a queue in front of a ticket counter during the so-called 'busy period' (say in the morning) and $\mathcal{A}$ represents the total serving time of the customers during the busy period. The same functional $\mathcal{A}$ also appears in the study of the distribution of avalanche sizes in the directed Abelian sandpile model [6, 7], of the area of staircase polygons in compact directed percolation [7–9] and of the collapse time of a ball bouncing on a noisy platform [10]. The case $n = -3/2$ appears in an interesting problem of estimating the distribution of the lifetime of a comet in the solar system (see e.g. [11] and the

J. Stat. Mech. (2020) 023202

discussion in [1]). The case $n = -1/2$ appears in the context of computing the distribution of the period of oscillation of an undamped particle in a random potential, such as the Sinai potential [12].

Given the multitude of applications for different choices of n, it is natural to ask whether one can compute the distribution $P_n(A|x_0)$ for arbitrary n. Our first main result in this paper is an exact solution for $P_n(A|x_0)$ for arbitrary $n > -2$, for which $P_n(A|x_0)$ is well behaved. As we show, $P_n(A|x_0)$ is given by the formula

$$P_n(A|x_0) = \frac{1}{\Gamma(\nu)} \left(\frac{\nu^2}{D}\right)^{\nu} \frac{x_0}{A^{\nu+1}} \exp\left(-\frac{\nu^2 x_0^{1/\nu}}{D\,A}\right), \qquad \nu = \frac{1}{n+2}, \tag{5}$$

where $\Gamma(\dots)$ is the gamma function. One can check that equation (5) perfectly agrees with all the known solutions for $n = 0$, $n = 1$, $n = -1/2$ and $n = -3/2$. As one can see from equation (5), a power-law tail at large A and an essential singular behavior at $A \to 0$ appear for all admissible n. In order to shed light on the nature of the essential singularity, we employ the optimal fluctuation method (OFM). The OFM has been successfully applied recently in several other problems, dealing with Brownian motion pushed to a large deviation regime by constraints [13–17]. Here we show that the OFM reproduces the essential singularity exactly by identifying the optimal, or most likely, path—a special trajectory of the Brownian motion that makes a dominant contribution to the PDF $P_n(A|x_0)$ at $A \to 0$. In particular, we find that, when $A \to 0$, the most likely value of the first-passage time t_f is finite for $-2 < n < 2$ and infinite for $n \geqslant 2$.

In the second part of this paper we study the same class of functionals as in equation (3), but for a Brownian motion with a nonzero constant drift,

$$\frac{\mathrm{d}x}{\mathrm{d}t} = -\mu + \eta(t), \tag{6}$$

starting at $x_0 > 0$. In equation (6), $\eta(t)$ is the same zero mean, delta-correlated Gaussian white noise as before, and μ describes the drift. If $\mu > 0$, the Brownian particle drifts toward the origin, while for $\mu < 0$ it drifts away from the origin. The relative magnitude of the drift and diffusion is described by the dimensionless Péclet number,

$$\mathrm{Pe} = \frac{\mu x_0}{2D}. \tag{7}$$

For $\mu > 0$ (drift toward the origin), the particle will surely cross the origin for the first time at a finite t_f, and we are again interested in the PDF $P_n(A|x_0)$ of the values A of the functional (3) for general n. It turns out that, for $\mu > 0$, this PDF is well behaved only for $n > -1$, as we explain below. For the case of $\mu < 0$, the Brownian particle escapes to infinity with a finite probability [3]. We briefly consider the case of $\mu < 0$ by conditioning the process on the non-escape.

For $\mu > 0$ the PDF $P_n(A|x_0)$ of the values of the functional (3) was studied previously only for $n = 0$, where $\mathcal{A}$ is the mean passage time itself [3], and $n = 1$, where $\mathcal{A}$ represents the area under the drifted Brownian motion [5, 10]. The case of $n = 0$ is exactly solvable and well known [3]. In the case of $n = 1$ it was possible to obtain an exact solution for the Laplace transform of $P_1(A|x_0)$ in terms of Airy functions [5, 10]. However, inverting this Laplace transform turned out to be extremely hard, and even extracting the asymptotic behavior of $P_1(A|x_0)$ was quite nontrivial and technical, in

J. Stat. Mech. (2020) 023202

particular for large A [5]. Several papers have been devoted to extracting the large A asymptotics and computing the moments of A for $n=1$ [18, 19]. For other $n>-1$ and $\mu>0$ there are no known exact solutions (not even in the Laplace space). This is an ideal situation where one can apply the OFM and obtain powerful new results. Here we take this course and obtain the exact leading-order asymptotic behaviors of $P_n(A|x_0)$ both at $A\to 0$ and $A\to\infty$, for arbitrary $n>-1$. In particular, we show that for $n\geqslant 0$ these asymptotics are given by the expressions

$$-\ln P_n(A|x_0)\simeq\begin{cases}\frac{1}{D}\frac{x_0^{n+2}}{(n+2)^2}\,\frac{1}{A}, & A\to 0,\\[2ex] \frac{\beta_n}{2D}\,\mu^{\frac{n+2}{n+1}}\,A^{\frac{1}{n+1}}, & A\to\infty,\end{cases}\tag{8}$$

where

$$\beta_n=(n+1)\left[\frac{\sqrt{\pi}\,2^{1-1/n}}{n+2}\,\frac{\Gamma(1+1/n)}{\Gamma(1/2+1/n)}\right]^{\frac{n}{n+1}}.\tag{9}$$

For $n=0$ equation (8) agree with the asymptotics extracted from the exact expression for $P_0(A|x_0)$ using the fact that $\lim_{n\to 0}\beta_n=1/2$ [3]. For $n=1$, they agree with those of [5, 18]. The $A\to 0$ asymptotic in equation (8) is valid for all $n>-1$, is independent of μ and agrees with the leading small-A behavior, equation (5), obtained for $\mu=0$. The large-A asymptotic in equation (8) is valid only for $n\geqslant 0$. For $-1<n<0$, the large-A tail of $P_n(A|x_0)$ presumably exhibits a power-law behavior which is beyond the accuracy of the OFM. The asymptotics (8) constitute the second main result of our paper.

In the weak noise limit, which corresponds to $\mathrm{Pe}\to\infty$, see equation (7), the OFM becomes asymptotically exact for all A. We show that in this limit $-\ln P_N(A)$ exhibits a large deviation scaling of the form

$$-\ln P_n(A)=\mathrm{Pe}\,\Phi_n\left(\frac{A}{\bar{A}}\right),\tag{10}$$

where

$$\bar{A}=\frac{x_0^{n+1}}{\mu(n+1)},\tag{11}$$

and we compute analytically, for any $n>-1$, the rate function $\Phi_n(z)$. When $n\geqslant 0$, the rate function vanishes only at its unique minimum point $z=1$, that is at $A=\bar{A}$, where $\bar{A}$ is the mean value of A in the limit of $\mathrm{Pe}\to\infty$. In this case $\Phi_n(z)$ has a quadratic behavior near the minimum point $z=1$, describing typical, Gaussian fluctuations of A. Furthermore, it diverges at $z\to 0$ and $z\to\infty$ leading to the asymptotic behaviors (8).

For $-1<n<0$ the behavior of $\Phi_n(z)$ changes dramatically. At $z<1$ the rate function $\Phi_n(z)$ continues to be nonzero, and its $z\to 0$ asymptotic corresponds to the $A\to 0$ asymptotic of equation (8). Remarkably, the rate function is equal to zero at all $z\geqslant 1$, and we uncover a dynamical phase transition at $z=1$. For $-1/2<n<0$ we obtain $\Phi_n(z)\sim(1-z)^2$ as $z\to 1$ from below, so this dynamical phase transition is of the

J. Stat. Mech. (2020) 023202

second order. However, for $-1 < n < -1/2$, we find $\Phi_n(z) \sim (1-z)^{1/(n+1)}$ as $z \to 1$ from below. Here the order of transition continuously depends on n and varies from 2 at $n \to -1/2$ to infinity at $n \to -1$. The order of transition is thus in general non-integer and even non-rational. This dynamical phase transition and, more generally, the exact rate function $\Phi_n(z)$ for all $n > -1$, alongside with the predicted optimal paths of the Brownian motion, conditioned on a specified A, constitute the third main result of this paper.

Finally, we employ the OFM to study the case of $\mu < 0$ (drift away from the origin), when the process is conditioned on reaching the origin. Here we show that the distribution of $\mathcal{A}$ coincides with the distribution of $\mathcal{A}$ for $\mu > 0$ with the same $|\mu|$.

The rest of the paper is organised as follows. In section 2 we consider the Brownian motion with zero drift. We first obtain, in section 2.1, $P_n(A|x_0)$ exactly for arbitrary $n > -2$. In section 2.2 we show how to obtain the small-A asymptotics of $P_n(A|x_0)$, and explain the essential singularity, by using the OFM. In section 3 we consider the Brownian motion with a drift toward the origin ($\mu > 0$). We start with presenting some exact results in the particular cases $n = 0$, 1 and 2. Then we show how one can apply the OFM in order to compute, in the limit of $\mathrm{Pe} \to \infty$, the exact rate function $\Phi_n(z)$ for all $n > -1$. In section 4 we reproduce our OFM results for $\Phi_n(z)$ by a different, albeit related method: applying a variant of WKB approximation to the exact equation for the Laplace transform of $P_n(A|x_0)$. We conclude with a summary and discussion in section 5. The case $\mu < 0$ is considered in the appendix.

2. Brownian motion with zero drift

2.1. Exact results

Here we consider the Brownian motion with zero drift as described by equation (1). In order to compute $P(A|x_0)$ for general $U(x)$, it is useful to consider its Laplace transform

$$Q_p(x_0) = \left\langle \mathrm{e}^{-p\,A} \right\rangle = \left\langle \mathrm{e}^{-p\int_0^{t_f} U(x(t))\,\mathrm{d}t} \right\rangle = \int_0^\infty P(A|x_0)\,\mathrm{e}^{-p\,A}\,\mathrm{d}A. \tag{12}$$

The angular brackets $\langle \dots \rangle$ denote averaging over all trajectories starting at x_0 (this averaging includes averaging over the history as well as over t_f itself). A nice property of this Laplace transform is that one can derive a linear second-order ordinary differential equation (ODE) for $Q_p(x_0)$ by treating the starting position x_0 as a variable. This is the 'backward' approach since one varies the position at the initial time. For a simple derivation of this equation we refer the readers to [1] (see also [5, 20]). The main idea, in words, is to evolve the trajectory from x_0 to a new starting position $x_0 + \mathrm{d}x_0$ in a small time interval $\mathrm{d}t$ and then keep track of how $Q_p(x_0)$ evolves as a result. Skipping details, one obtains

$$D\,\frac{\mathrm{d}^2 Q_p}{\mathrm{d}x_0^2} - p\,U(x_0)\,Q_p(x_0) = 0\,, \tag{13}$$

valid for $x_0 \geqslant 0$, with the boundary conditions:

$$\text{(i)} \quad Q_p(x_0 = 0) = 1 \quad \text{and} \quad \text{(ii)} \quad Q_p(x_0 \to \infty) \to 0. \tag{14}$$

The condition (i) stems from the fact that in this case $t_f = 0$ for a well behaved $U(x)$, and hence $\langle \mathrm{e}^{-p \int_0^{t_f} U(x(t))\,\mathrm{d}t} \rangle \to 1$ as $x_0 \to 0$. The condition (ii) follows from the fact that, as $x_0 \to \infty$, $t_f \to \infty$ as well. When A is kept fixed, the resulting PDF $P(A|x_0)$, and its Laplace transform $Q_p(x_0)$, must vanish.

Notice that equation (13) is different from the Feynman–Kac equation: the latter is a partial differential equation that involves time explicitly (since it deals with functionals over a fixed time interval). In our case, since one sums over all possible trajectories with different first-passage times, there is no explicit time dependence in the equation for $Q_p(x_0)$.

Equation (13) can be viewed as a Schrödinger equation (with a bit unusual boundary condition (14)(i) for the 'wave function') for a zero-energy particle, and solving it for arbitrary potential $U(x_0)$ is not possible. Fortunately, for our choice $U(x) = x^n$, as in equation (3), the solution can be obtained in a closed form. Here equation (13) becomes

$$D\,\frac{\mathrm{d}^2 Q_p}{\mathrm{d}x_0^2} - p\,x_0^n\,Q_p(x_0) = 0\,. \tag{15}$$

This equation has two linearly independent solutions

$$q_1(x_0) = \sqrt{x_0}\,I_\nu\left(2\nu\sqrt{\frac{p}{D}}\,x_0^{\frac{1}{2\nu}}\right) \quad \text{and} \quad q_2(x_0) = \sqrt{x_0}\,K_\nu\left(2\nu\sqrt{\frac{p}{D}}\,x_0^{\frac{1}{2\nu}}\right), \tag{16}$$

where $\nu = 1/(n+2)$, $I_\nu(\dots)$ and $K_\nu(\dots)$ are the modified Bessel functions of the first and second kind [21, 22], respectively, and we assumed $n > -2$ strictly[3]. As $x_0 \to \infty$, $q_1(x_0)$ diverges, while $q_2(x_0)$ tends to zero. Therefore, $q_1(x_0)$ should be discarded. The solution $q_2(x_0)$ is well-behaved at $x_0 \to 0$. Normalizing it so as to obey the boundary condition (14) (i), we arrive at the desired Laplace transform

$$Q_p(x_0) = \frac{2\nu^\nu}{\Gamma(\nu)\,D^{\nu/2}}\,p^{\nu/2}\,\sqrt{x_0}\,K_\nu\left(2\,\nu\,\sqrt{\frac{p}{D}}\,x_0^{\frac{1}{2\nu}}\right), \qquad \nu = \frac{1}{n+2}, \quad n > -2. \tag{17}$$

The inversion of this Laplace transform looks challenging, but we succeeded in performing it by virtue of the following identity [22]:

$$\int_0^\infty \mathrm{d}z\,z^{-\nu-1}\,\mathrm{e}^{-p\,z-\frac{\gamma}{z}} = 2\left(\frac{p}{\gamma}\right)^{\nu/2} K_\nu\left(2\sqrt{\gamma p}\right). \tag{18}$$

Consequently, the Laplace inversion

$$\mathcal{L}_p^{-1}\left[p^{\nu/2}\,K_\nu(2\sqrt{\gamma p})\right] = \frac{1}{2}\,\gamma^{\nu/2}\,A^{-\nu-1}\,\mathrm{e}^{-\gamma/A}\,. \tag{19}$$

Hence, using the identity (19) and choosing $\gamma = (\nu^2/D)\,x_0^{1/\nu}$, one can invert equation (17) and get an exact expression for our distribution $P_n(A|x_0)$, valid for all $A > 0$ and $x_0 \geqslant 0$, once $n > -2$:

[3] For $n \leqslant -2$ and $p > 0$, the only solution of equation (15) that satisfies the boundary condition $Q_p(x_0 \to \infty) = 0$ is $Q_p(x_0) = 0$ leading to $\mathcal{A} = \infty$.

J. Stat. Mech. (2020) 023202

$$P_n(A|x_0) = \frac{1}{\Gamma(\nu)} \left(\frac{\nu^2}{D}\right)^{\nu} \frac{x_0}{A^{\nu+1}} \exp\left(-\frac{\nu^2}{D\,A}\, x_0^{1/\nu}\right), \qquad \nu = \frac{1}{n+2}\,. \tag{20}$$

One can check that $P_n(A|x_0)$ is normalized to unity, $\int_0^\infty P_n(A|x_0)\,\mathrm{d}A = 1$. Also, for $n = -3/2$, $-1/2$, 0 and 1, it reduces to the known results. As one can see, the A-dependence of $P_n(A|x_0)$ in equation (20) is given by a product of just two factors: the power-law factor $A^{-\nu-1}$ that describes the large-A decay and the factor $\exp\left(-\frac{\nu^2 x_0^{1/\nu}}{DA}\right)$, which determines the much faster small-A decay and exhibits an essential singularity at $A \to 0$. The power-law factor $A^{-\nu-1}$ can be obtained by the following scaling argument. Noting that for a Brownian motion one has $x(t) \sim t^{1/2}$ for large t, one obtains for large t_f

$$\mathcal{A} = \int_0^{t_f} [x(t)]^n\,\mathrm{d}t \sim t_f^{(n+2)/2}\,. \tag{21}$$

Now, the distribution of the first-passage time t_f for large t_f scales as $P_0(t_f|x_0) \sim x_0\, t_f^{-3/2}$, see equation (4). Hence, using $P_0(t_f|x_0)\,\mathrm{d}t_f = P_n(A|x_0)\,\mathrm{d}A$ and plugging the scaling relation into equation (21), we obtain $P_n(A|x_0) \sim x_0\, A^{-\nu-1} = x_0\, A^{-(n+3)/(n+2)}$ for $A \to \infty$[4].

This scaling argument however fails to account for the essentially-singular small-A behavior, since one can no longer use the scaling relation (21) for small A. This large-deviation-type behavior, however, is perfectly captured by the optimal fluctuation method as we now demonstrate.

2.2. Optimal fluctuation method explains essential singularity at $A \to 0$

When applied to the Brownian motion, the OFM essentially becomes geometrical optics [13–17]. A natural starting point of the OFM is the probability of a Brownian path $x(t)$, which is given, up to pre-exponential factors, by the Wiener's action, see e.g. [1]:

$$-\ln P = S = \frac{1}{4D}\int_0^{t_f} \dot{x}^2(t)\,\mathrm{d}t. \tag{22}$$

The distribution $P_n(A|x_0)$ can then be written as $P_n(A|x_0) = \langle \delta(A - \mathcal{A})\rangle$ where, as in equation (12), the angular brackets denote an average over all Brownian trajectories, starting at x_0 and reaching the origin for the first time at t_f, as well as over all possible values of t_f. The delta-function can be replaced by its integral representation:

$$P_n(A|x_0) = \langle \delta(\mathcal{A} - A)\rangle = \left\langle \frac{1}{2D}\int \frac{\mathrm{d}\lambda}{2\pi i} \exp\left[\frac{\lambda}{2D}(\mathcal{A} - A)\right]\right\rangle, \tag{23}$$

where the integration over λ is along the vertical axis (the Bromwich contour) in the complex λ plane. This extra piece, added to the Wiener measure in equation (22), gives rise to an effective action functional

$$S_{\mathrm{eff}} = \frac{1}{2D}\left[\frac{1}{2}\int_0^{t_f} \dot{x}^2(t)\,\mathrm{d}t - \lambda\left(\int_0^{t_f} [x(t)]^n \mathrm{d}t - A\right)\right]. \tag{24}$$

[4] It follows from equation (20) that the mean value of $\mathcal{A}$ is finite for $-2 < n < -1$ and infinite for $n > -1$.

J. Stat. Mech. (2020) 023202

Thus, one can interpret λ as the Lagrange multiplier that enforces the constraint $\mathcal{A} = A$. In the regime when the effective action $S_{\rm eff}$ is very large, the leading-order contribution to $P_n(A|x_0)$ can be obtained by the saddle point method. This requires minimizing $S_{\rm eff}$ from equation (24) (i) over all trajectories $x\,(t)$ that start at x_0, satisfy the condition $x(t) > 0$ for $0 < t < t_f$, and arrive at $x = 0$ at time t_f, (ii) over all possible values of t_f, and (iii) over λ so as to impose the constraint $\mathcal{A} = A$. It is convenient to think of $S_{\rm eff}$ as of the action of a Newtonian particle of unit mass with the time-independent Lagrangian

$$L_\lambda\,(x, \dot{x}) = \frac{\dot{x}^2}{2} + \lambda x^n, \tag{25}$$

where the first terms describes the kinetic energy, and the second term corresponds to the effective potential $V(x) = -\lambda\, x^n$. The extremal is described by the Euler–Lagrange equation

$$\ddot{x}(t) - \lambda n x^{n-1}(t) = 0. \tag{26}$$

Having solved this equation subject to all constraints, we will obtain the optimal (most likely) path of our constrained Brownian motion. The first integral of equation (26) describes conservation of energy:

$$\frac{\dot{x}^2}{2} - \lambda\, x^n = E\,, \quad 0 \leqslant t \leqslant t_f \tag{27}$$

where the energy E is a constant of motion. To determine E, we minimize $S_{\rm eff}$ in equation (24) with respect to t_f at fixed x_0 and λ and obtain

$$\left(\frac{\dot{x}^2}{2} - \lambda x^n\right)\Big|_{t=t_f} = 0\,. \tag{28}$$

Comparing equations (27) and (28), we obtain $E = 0$, so that

$$\frac{\dot{x}^2}{2} = \lambda\, x^n\,, \quad 0 \leqslant t \leqslant t_f. \tag{29}$$

By virtue of equation (29), the effective action in equation (24), evaluated on the optimal path, is equal to

$$S_{\rm opt} = S_{\rm eff}\big|_{\rm optimal\ path} = \frac{\lambda A}{2D}. \tag{30}$$

To express λ via A and x_0, we have to integrate equation (29) and obtain the optimal path $x(t)$, satisfying the required constraints. From equation (29) we obtain

$$\dot{x} = -\sqrt{2\lambda}\, x^{n/2}. \tag{31}$$

The equation with the plus sign, $\dot{x} = \sqrt{2\lambda}\, x^{n/2}$, must be discarded because it would drive the path to infinity and lead to $\mathcal{A} = \infty$ for all n. Some of the further details of the optimal path depend on whether $-2 < n < 2$, $n > 2$, or $n = 2$, as we will now see.

2.2.1. $n > 2$. The solution of equation (31) that obeys the initial condition $x(0) = x_0$, can be written as

$$x(t) = \left[x_0^{1-\frac{n}{2}} + \frac{\sqrt{\lambda}(n-2)t}{\sqrt{2}} \right]^{-\frac{2}{n-2}}. \tag{32}$$

Here the optimal path approaches zero only at $t \to \infty$. That is, the optimal value of the first-passage time $t_f = \infty$. The constraint (3) (with time integration extended to infinity) yields

$$\lambda = \frac{2x_0^{n+2}}{A^2(n+2)^2}, \tag{33}$$

so the optimal path, for specified x_0 and A, is

$$x(t) = x_0 \left[1 + \frac{(n-2)x_0^n t}{(n+2)A} \right]^{-\frac{2}{n-2}}. \tag{34}$$

Plugging λ from equations (33) into (30), we get

$$S_{\rm opt} = \frac{x_0^{n+2}}{(n+2)^2 DA}. \tag{35}$$

As a result,

$$P_n(A|x_0) \sim \exp(-S_{\rm opt}) = \exp\left[-\frac{x_0^{n+2}}{(n+2)^2 DA} \right], \tag{36}$$

and we must demand $S_{\rm opt} \gg 1$ to justify the saddle point evaluation of the path integral. Equation (36) correctly reproduces the leading-order singular behavior of the exact result in equation (20). This happens when $A \to 0$ at fixed x_0 and D, or for any A when $Dx_0^{-(n+2)} \to 0$.

2.2.2. $-2 < n < 2$. Here equation (32) continues to hold, but the optimal solution $x(t)$ has a compact support $0 \leqslant t < t_f$, where t_f is a finite optimal first-passage time. In terms of λ

$$t_f = \frac{\sqrt{2}\, x_0^{1-\frac{n}{2}}}{\sqrt{\lambda}\,(2-n)}. \tag{37}$$

The constraint (3), with integration from 0 to t_f, again yields equations (33) and (34) (where $0 \leqslant t \leqslant t_f$) and equations (35) and (36), in full agreement with the leading small-A behavior of $P_n(A|x_0)$ in equation (20). In terms of A the optimal first-passage time (37) is

$$t_f = \frac{(n+2)A}{(2-n)x_0^n}, \quad -2 < n < 2. \tag{38}$$

In the particular case $n = 1$ the optimal path (34) is a parabola

$$x(t) = \frac{x_0(3A - x_0 t)^2}{9A^2}, \quad 0 \leqslant t \leqslant t_f = \frac{3A}{x_0}. \tag{39}$$

J. Stat. Mech. (2020) 023202

The parabola is tangent to the t-axis at $t = t_f$. For $n = 0$ the optimal path (34) is a straight line:

$$x(t) = x_0 \left(1 - \frac{t}{A}\right), \quad 0 \leqslant t \leqslant t_f \equiv A. \tag{40}$$

2.2.3. $n = 2$. In the special case $n = 2$, the solution of equation (31), conditioned on x_0 and A, is

$$x(t) = x_0 \, \mathrm{e}^{-\frac{x_0^2 t}{2A}}, \tag{41}$$

so that the optimal first passage time is infinite. Here $\lambda = x_0^2/(8A^2)$, and the optimal action is described by equation (35) and, again, correctly describes the singular behavior of exact $P_2(A|x_0)$ from equation (35) with $n = 2$ at $A \to 0$.

3. Brownian motion in the presence of drift

3.1. Exact results

Here we consider the Brownian motion in the presence of a nonzero drift μ which can be described by equation (6). We are again interested in the PDF $P(A|x_0)$ of the first-passage functionals of the type $\mathcal{A} = \int_0^{t_f} U(x(t))\,\mathrm{d}t$. Following the same line of arguments as in the driftless case [5, 20], one can obtain, for arbitrary $U(x)$, a second-order ODE for the Laplace transform, $Q_p(x_0) = \int_0^\infty \mathrm{e}^{-pA} P(A|x_0)\,\mathrm{d}A$:

$$D\,\frac{\mathrm{d}^2 Q_p}{\mathrm{d}x_0^2} - \mu\,\frac{\mathrm{d}Q_p}{\mathrm{d}x_0} - p\,U(x_0)\,Q_p(x_0) = 0\,. \tag{42}$$

The boundary conditions (14) continue to hold. For our choice $U(x) = x^n$ equation (42) becomes

$$D\,\frac{\mathrm{d}^2 Q_p}{\mathrm{d}x_0^2} - \mu\,\frac{\mathrm{d}Q_p}{\mathrm{d}x_0} - p\,x_0^n\,Q_p(x_0) = 0\,. \tag{43}$$

Unlike for $\mu = 0$, where exact solutions could be derived for arbitrary $n > -2$, for $\mu > 0$ we are aware of only three exactly solvable cases for equation (43): $n = 0$, 1 and 2, so let us briefly consider them.

3.1.1. $n = 0$. Here $A = t_f$, and the solution of equation (43) with the boundary conditions (14) is elementary [5, 20]:

$$Q_p(x_0) = \exp\left(\frac{\mu x_0}{2D} - \frac{x_0}{\sqrt{D}}\sqrt{\frac{\mu^2}{4D} + p}\right). \tag{44}$$

This Laplace transform can be readily inverted to give the well-known exact distribution of the first-passage time [3]

J. Stat. Mech. (2020) 023202

$$P_0(t_f|x_0) = \frac{x_0}{\sqrt{4\,\pi\,D\,t_f^3}}\,\exp\left[-\frac{1}{4\,D\,t_f}\,(x_0-\mu\,t_f)^2\right]\,, \tag{45}$$

which is a simple extension of the driftless result (4).

3.1.2. $n = 1$. In this case, studied in [5], one obtains

$$Q_p(x_0) = \int_0^\infty P_1(A|x_0)\,\mathrm{e}^{-p\,A}\,\mathrm{d}A = \frac{\mathrm{e}^{\frac{\mu x_0}{2D}}\,\mathrm{Ai}\left(\frac{\mu^2+4pDx_0}{4p^{2/3}D^{4/3}}\right)}{\mathrm{Ai}\left(\frac{\mu^2}{4p^{2/3}D^{4/3}}\right)}, \tag{46}$$

where $\mathrm{Ai}(z)$ is the Airy function. Inverting this Laplace transform exactly does not seem feasible. Even extracting the asymptotic behaviors of $P_1(A|x_0)$ for large A from this Laplace transform is nontrivial. This was done in [5] by employing a rather technical method (see also [18]). In contrast, the small-A behavior is easy to derive as it effectively corresponds to the driftless case. The asymptotic behaviors of $P_1(A|x_0)$ are given by [5]

$$P_1(A|x_0) \simeq \begin{cases} \frac{x_0}{\Gamma(1/3)(9D)^{1/3}}\,A^{-4/3}\,\exp\left(-\frac{x_0^3}{9\,D\,A}\right), & A\to 0, \\ \left(\frac{2}{3}\right)^{1/4}\frac{x_0}{\sqrt{\pi}\,(2D)^{3/2}}\,\mu^{7/4}\,A^{-3/4}\,\exp\left(-\sqrt{\frac{2}{3}}\,\frac{\mu^{3/2}}{D}\,\sqrt{A}\right), & A\to\infty, \end{cases} \tag{47}$$

where the leading-order $A \to 0$ asymptotic coincides with the corresponding asymptotic in equation (8) for $n = 1$.

3.1.3. $n = 2$. To our knowledge, this case has not been studied before. The general solution of equation (43) can be represented as a linear combination of two independent solutions, one of which decaying at infinity, and the other growing without limit. In view of the boundary condition (14) at $x_0 \to \infty$, the growing solution must be discarded. The remaining arbitrary constant is chosen so that the solution obeys the boundary condition (14) at $x_0 = 0$. Skipping details, we just present the solution for $Q_p(x_0)$:

$$Q_p(x_0) = \mathrm{e}^{\frac{\mu x_0}{2D}}\,\frac{D_q\left[\left(\frac{4p}{D}\right)^{1/4}\,x_0\right]}{D_q(0)}, \quad \text{where} \quad q = -\frac{1}{2} - \frac{\mu^2}{8D^{3/2}\sqrt{p}}\,, \tag{48}$$

and $D_q(z)$ is the parabolic cylinder function [21]; note that $D_q(0) = \sqrt{\pi}\,2^{q/2}/\Gamma[(1-q)/2]$. Inverting the Laplace transform (48) exactly looks hopeless. Once again, while the leading small-A behavior coincides with the one in the driftless case, extracting the large A asymptotics is not easy.

We are unaware of any other case except $n = 0$, 1 and 2, when equation (43) with the boundary conditions (14) can be solved exactly. That is, not even the Laplace transform can be determined exactly. As we will now see, here comes the real power of the OFM. But before employing the OFM, we present one more exact result: for the mean value of the random variable $\mathcal{A} = \int_0^{t_f} x^n(t)\,\mathrm{d}t$ for any $n > -1$.

Exact mean. In terms of the Laplace transform $Q_p(x_0)$, the mean is given by

J. Stat. Mech. (2020) 023202

$$\langle \mathcal{A} \rangle \equiv m_1(x_0) = \left\langle \int_0^{t_f} x^n(t)\, \mathrm{d}t \right\rangle = -\frac{\mathrm{d}Q_p(x_0)}{\mathrm{d}p}\Big|_{p=0}, \tag{49}$$

where $Q_p(x_0)$ satisfies equation (43). Taking the derivative of equation (43) with respect to p and setting $p = 0$, we obtain a simple differential equation for $m_1(x_0)$:

$$D\,\frac{\mathrm{d}^2 m_1(x_0)}{\mathrm{d}x_0^2} - \mu\,\frac{\mathrm{d}m_1(x_0)}{\mathrm{d}x_0} = -x_0^n\,. \tag{50}$$

It has to be solved subject to the following boundary conditions: (i) $m_1(x_0 = 0) = 0$ and (ii) $m_1(x_0)$ cannot grow faster than a power law as $x_0 \to \infty$. The solution is straightforward, and we obtain, for $n > -1$,

$$m_1(x_0) = \frac{1}{D}\int_0^{x_0} \mathrm{d}x\, \mathrm{e}^{\mu x/D} \int_x^{\infty} y^n\, \mathrm{e}^{-\mu y/D}\, \mathrm{d}y\,. \tag{51}$$

Evaluating the double integral, we arrive at the exact result

$$\begin{aligned} m_1(x_0) &= \frac{1}{\mu}\left\{ \frac{{x_0}^{n+1}}{n+1} + \left(\frac{D}{\mu}\right)^{n+1} \left[\mathrm{e}^{\mu x_0/D}\,\Gamma\left(n+1, \frac{\mu\, x_0}{D}\right) - \Gamma(n+1)\right]\right\} \\ &= \bar{A}\left\{1 + \frac{1}{\mathrm{Pe}^{n+1}}\frac{n+1}{2^{n+1}}\left[\mathrm{e}^{2\mathrm{Pe}}\Gamma\left(n+1, 2\mathrm{Pe}\right) - \Gamma(n+1)\right]\right\}, \quad n > -1, \end{aligned} \tag{52}$$

where $\Gamma(n+1, z) = \int_z^{\infty} \mathrm{e}^{-u}\, u^n\, \mathrm{d}u$ is the incomplete gamma function, and $\bar{A}$ is defined in equation (11). Note that, as Pe tends to infinity, the function $\mathrm{e}^{2\mathrm{Pe}}\Gamma\left(n+1, 2\mathrm{Pe}\right)$ behaves as $2^n\mathrm{Pe}^n$. As a result, the exact mean value $m_1(x_0)$ approaches $\bar{A}$ from equation (11) as $1/\mathrm{Pe}$ when $\mathrm{Pe} \to \infty$[5].

By taking higher derivatives of $Q_p(x_0)$ with respect to p and setting $p = 0$ one can derive differential equations for higher moments and, in principle, solve them recursively. However, this recursive procedure, beyond the first moment, quickly becomes complicated. In addition, it does not shed light on the tails of the distribution $P_n(A|x_0)$. We will show now how to obtain the distribution tails by using the OFM.

3.2. Optimal fluctuation method

By virtue of the Langevin equation (6), the probability of an unconstrained path $x\,(t)$ is now given by

$$-\ln P = S = \frac{1}{4D}\int_0^{t_f} (\dot{x} + \mu)^2\, \mathrm{d}t\,. \tag{53}$$

As in the driftless case in equation (24), taking into acount the constraint $\mathcal{A} = A$ gives rise to an effective action

$$S_{\mathrm{eff}} = \frac{1}{2D}\left[\frac{1}{2}\int_0^{t_f} (\dot{x} + \mu)^2\, \mathrm{d}t - \lambda\left(\int_0^{t_f} [x(t)]^n \mathrm{d}t - A\right)\right], \tag{54}$$

[5] As one can check from equation (52), $m_1(x_0)$ diverges in the driftless case $\mu = 0$, or $\mathrm{Pe} = 0$, in agreement with our driftless result of section 2.1 for $n > -1$.

J. Stat. Mech. (2020) 023202

where λ is the Lagrange multiplier. Again, we assume *a priori* that there is a regime where $S_{\rm eff}$ is large and hence $P_n(A|x_0)$ can then be estimated by the saddle point method. This again means minimizing $S_{\rm eff}$ with respect to (i) all trajectories starting at x_0 at $t=0$ and ending at $x=0$ at $t=t_f$ while staying positive in between, (ii) all possible values of t_f, and (iii) all λ so as to impose the constraint $\mathcal{A}=A$. Once the optimal path is found, the distribution $P_n(A|x_0)$ can be evaluated from the optimal action

$$-\ln P_n(A|x_0) \simeq S_{\rm opt} = S_{\rm eff}\Big|_{\rm optimal\,path}. \tag{55}$$

The presence of the μ-term alters neither the Euler–Langrange equation,

$$\ddot{x}(t) - \lambda n x^{n-1}(t) = 0, \tag{56}$$

nor the energy integral

$$\frac{\dot{x}^2}{2} - \lambda x^n = E = \text{const.} \tag{57}$$

For zero drift, the energy E was zero. For $\mu>0$, it will be nonzero as we will see shortly. As in the driftless case, E is determined from minimizing $S_{\rm eff}$ in equation (54) with respect to t_f for fixed x_0 and λ. This minimization gives a condition that we will use shortly:

$$\frac{1}{2}\left(\dot{x}+\mu\right)^2\Big|_{t=t_f} - \lambda x^n(t_f) = 0. \tag{58}$$

Before proceeding further, let us remark that for $\lambda=0$ the process is unconstrained, and the optimal path—the ballistic trajectory

$$x(t) = x_0 - \mu t \tag{59}$$

—is unaffected by the noise. In this case

$$\mathcal{A} = \int_0^{x_0/\mu} (x_0-\mu t)^n\,{\rm d}t = \frac{x_0^{n+1}}{\mu\,(n+1)} = \bar{A}, \qquad n>-1, \tag{60}$$

where $\bar{A}$ is defined in equation (11). This is thus the mean value of $\mathcal{A}$ in the limit of ${\rm Pe}\to\infty$, as we also obtained from the exact result (52). Let us first consider the case $n>0$, where equations (57) and (58) suffice to determine the energy E of the effective Newtonian particle.

3.2.1. $n>0$. In this case $x^n(t_f)=0$, and it follows from equation (58) that

$$\dot{x}\big|_{t=t_f} = -\mu\,. \tag{61}$$

Then, using equation (57) at $t=t_f$, we obtain $E=\mu^2/2$. As a result,

$$\frac{\dot{x}^2}{2} - \lambda x^n(t) = \frac{\mu^2}{2} \qquad \text{for } n>0 \quad \text{and} \quad 0\leqslant t\leqslant t_f. \tag{62}$$

Once the energy is fixed, the optimal path $x(t)$ and the optimal first-passage time t_f can be determined by integrating the first-order ODE (62) with the boundary conditions $x(0)=x_0$ and $x(t_f)=0$, while λ is set up by the constraint $\mathcal{A}=A$. For a general $n>0$

J. Stat. Mech. (2020) 023202

the optimal path cannot be expressed in explicit form. However, it is possible to evaluate the optimal action $S_{\rm opt}$ as a function of A in a parametric form, where the Lagrange multiplier plays the role of the parameter.

Let us first express the effective action in equation (54) for the optimal path as a function of A and t_f. Expanding $(\dot{x}+\mu)^2$ and using equation (62) and the condition $x(t_f)=0$, we obtain

$$S_{\rm opt} = \frac{1}{2D}\left(-\mu\, x_0 + \mu^2\, t_f + \lambda\, A\right)\,. \tag{63}$$

When $\mu = 0$ equation (63) reduces to equation (30) for the driftless case. Our goal now is to express A and the optimal value of t_f in terms of λ and the parameters D, μ and x_0. The nature of the optimal trajectory depends on the parameter λ. Consider first $\lambda > 0$, where the effective potential $V(x) = -\lambda x^n$ is negative for all $x > 0$. Here the effective Newtonian particle with fixed energy $E = \mu^2/2$, that starts at $x_0 > 0$ can reach $x = 0$ only if it moves monotonically toward 0. The situation is different for $\lambda < 0$. Note that the λ cannot be arbitrarily negative, since that the particle energy $E = \mu^2/2$ cannot be smaller that its potential energy. Using equation (62) at $t = 0$, we see that λ cannot be smaller than $-\lambda_c$, where

$$\lambda_c = \frac{\mu^2}{2\, x_0^n}\,. \tag{64}$$

Now consider $-\lambda_c \leqslant \lambda < 0$. In this case, the potential $V(x) = -\lambda x^n$ is positive for $x > 0$, and there are two possible solutions for $x(t)$ with the same λ: a monotone decreasing one and a non-monotone one. For the non-monotone solution $x(t)$ first increases until it reaches the reflection point $x_m = (2\mu^2/|\lambda|)^{\,1/n}$, where $\dot{x} = 0$, gets reflected and decreases to zero. For the same λ the non-monotone solution yields a larger value of A than the monotone one. Figure 1 depicts the dependence of A on λ, which is described by equations (71) and (81) below, in the particular case of $n = 1$. One can see the lower branch of the $A(\lambda)$-dependence (branch 1), and the upper branch (branch 2). We now compute the optimal action (63) separately for branches 1 and 2.

Branch 1: $-\lambda_c < \lambda < +\infty$. Here we have only monotone trajectories with $\dot{x} < 0$, see the left panel of figure 2. Hence, from equation (62), taking the negative root, we have

$$\frac{{\rm d}x}{{\rm d}t} = -\sqrt{2\,\lambda\, x^n + \mu^2}. \tag{65}$$

Integrating this ODE from $t = 0$ to $t = t_f$ subject to $x(0) = x_0$ and $x(t_f) = 0$, we obtain

$$t_f = \int_0^{x_0} \frac{{\rm d}x}{\sqrt{2\lambda x^n + \mu^2}}. \tag{66}$$

It is convenient to define the dimensionless parameter

$$a = \frac{\lambda}{\lambda_c}\,. \tag{67}$$

For branch 1 we have $-1 < a < +\infty$. Rescaling $x = x_0\, u$ in equation (66), we obtain

$$t_f = \frac{x_0}{\mu}\int_0^1 \frac{{\rm d}u}{\sqrt{1+a\,u^n}} = \frac{x_0}{\mu}\;{}_2F_1(1/2, 1/n, 1+1/n, -a)\,; \quad -1 < a < \infty, \quad n > 0 \tag{68}$$

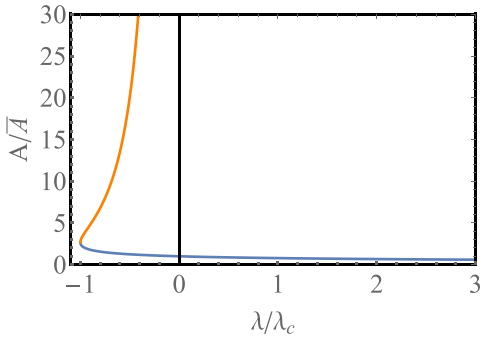

Figure 1. $A/\bar{A}$ versus λ/λ_c, as described by equations (71) and (81) for $n=1$. For fixed $\lambda>0$ there is only one solution for the optimal path $x(t)$ and A, corresponding to the lower branch (branch 1). For $-\lambda_c<\lambda<0$ there are two solutions, corresponding to the lower and upper branches (branches 1 and 2), denoted by the blue and orange lines, respectively.

where ${}_2F_1(a,b,c,z)$ is the hypergeometric function [22]. Now we express A via a from equation (67):

$$A=\int_0^{t_f} x^n(t)\,\mathrm{d}t=\int_0^{x_0} x^n(t)\left|\frac{\mathrm{d}t}{\mathrm{d}x}\right|\mathrm{d}x=\int_0^{x_0}\frac{x^n\,\mathrm{d}x}{\sqrt{2\lambda x^n+\mu^2}}\,. \tag{69}$$

This can be recast as

$$A=\frac{x_0^{n+1}}{\mu}\int_0^1\frac{u^n\,\mathrm{d}u}{\sqrt{1+a\,u^n}}=\frac{x_0^{n+1}}{\mu\,(n+1)}\,{}_2F_1(1/2,1+1/n,2+1/n,-a)\,;\quad -1<a<\infty. \tag{70}$$

For $a=0$ equations (68) and (70) yield the unconstrained (noiseless) values $t_f=x_0/\mu$, and $A=\bar{A}$ from equation (60), respectively. Introducing the dimensionless variable $z=A/\bar{A}$, we rewrite equation (70) as

$$z=\frac{A}{\bar{A}}={}_2F_1(1/2,1+1/n,2+1/n,-a)\,. \tag{71}$$

The limiting value $a=-1$ corresponds to

$$z_c=z(a=-1)={}_2F_1(1/2,1+1/n,2+1/n,1)=\sqrt{\pi}\,\frac{\Gamma(2+1/n)}{\Gamma(3/2+1/n)}\,. \tag{72}$$

Hence branch 1 is valid for $0<z\leqslant z_c$. Plugging the expressions for t_f from equation (68) and $z=A/\bar{A}$ from equations (71) into (63), we see that $S_{\rm opt}$ can be written in the scaling form

$$S_{\rm opt}=\mathrm{Pe}\,\Phi_n^{(1)}\left(\frac{A}{\bar{A}}\right)\,, \tag{73}$$

where the scaling function for branch 1, $\Phi_n^{(1)}(z)$, is given in a parametric form by the equations

J. Stat. Mech. (2020) 023202

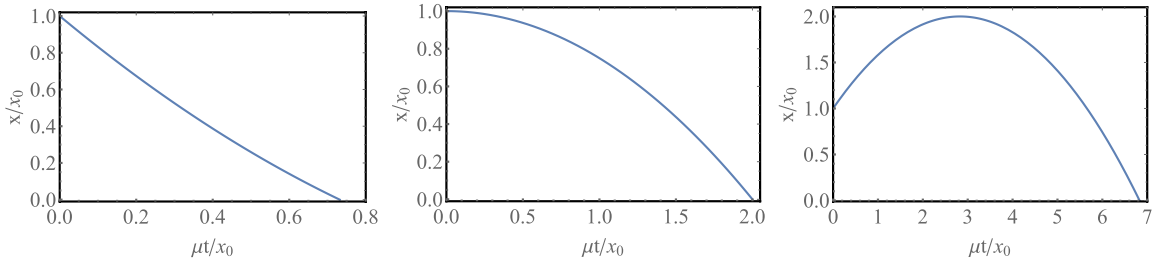

Figure 2. Examples of the optimal paths $x(t)$ corresponding to the branch 1 (the left panel) and branch 2 (the right panel), see the main text. At $\lambda = -\lambda_c$ (the middle panel) $\dot{x}$ vanishes at $t = 0$. In these examples $n = 1$, so that $x(t)$ is a parabola.

$$\begin{aligned} z &= {}_2F_1(1/2, 1+1/n, 2+1/n, -a), \\ \Phi_n^{(1)} &= -1 + {}_2F_1(1/2, 1/n, 1+1/n, -a) + \frac{a}{2(n+1)}\, z(a)\,, \end{aligned} \tag{74}$$

with the parameter $-1 \leqslant a < \infty$. The limiting behaviors of $\Phi_n^{(1)}(z)$ as $z \to 0$ (that is, $a \to \infty$) and $z \to 1$ (that is, $a \to 0$) are the following:

$$\Phi_n^{(1)}(z) \simeq \begin{cases} \frac{2(n+1)}{(n+2)^2 z}, & z \to 0. \\ \\ \frac{(2n+1)}{2\,(n+1)^2}\,(z-1)^2, & z \to 1. \end{cases} \tag{75}$$

Plugging the $z \to 0$ asymptotic from equations (75) in (73) and using equation (55) leads to the first line of equation (8) of the Introduction; it is independent of the drift μ. In its turn, the $z \to 1$ asymptotic in equation (75) describes a Gaussian behavior of $P_n(A|x_0)$ near its mean value $A = \bar{A}$:

$$-\ln P_n(A|x_0) = S_{\rm opt}\left(|A-\bar{A}| \ll \bar{A}\right) \simeq \frac{(2n+1)\mu^3}{4Dx_0^{2n+1}}\left(A-\bar{A}\right)^2\,, \tag{76}$$

with the variance $\sigma^2 = 2\,D\,x_0^{2n+1}/(2n+1)\mu^3$. Notice that $\sigma/\bar{A}$ scales as $1/\sqrt{\rm Pe}$, as to be expected for small Gaussian fluctuations.

Branch 2: $-\lambda_c < \lambda < 0$**.** Here t_f and A come from two trajectory segments (see the right panel of figure 2), which are governed by the equations

$$\frac{{\rm d}x}{{\rm d}t} = \sqrt{2\,\lambda\,x^n + \mu^2}\,, \qquad 0 < t < t_m, \tag{77}$$

$$\frac{{\rm d}x}{{\rm d}t} = -\sqrt{2\,\lambda\,x^n + \mu^2}\,, \quad 0 < t < t_m, \tag{78}$$

where t_m is the reflection time of the Newtonian particle from $x = x_m = (2\mu^2/|\lambda|)^{1/n}$. We obtain

$$t_f = \int_{x_0}^{x_m} \frac{{\rm d}x}{\sqrt{2\lambda x^n + \mu^2}} + \int_0^{x_m} \frac{{\rm d}x}{\sqrt{2\lambda x^n + \mu^2}}\,. \tag{79}$$

Using the same notation and rescalings as for the branch 1 (but $-1 < a < 0$ now), we can rewrite equation (79) as

$$t_f = \frac{x_0}{\mu}\left[\int_1^{(-a)^{-1/n}} \frac{\mathrm{d}u}{\sqrt{1+a\,u^n}} + \int_0^{(-a)^{-1/n}} \frac{\mathrm{d}u}{\sqrt{1+a\,u^n}}\right] = \frac{x_0}{\mu}\frac{2B(1/n,1/2) - B_{-a}(1/n,1/2)}{n(-a)^{1/n}}\,, \tag{80}$$

where $B_x[a,b] = \int_0^x y^{a-1}\,(1-y)^{b-1}\,\mathrm{d}y$ is the incomplete beta function (with $x \leqslant 1$) and $B[a,b] = B_1[a,b]$ is the standard beta function [22].

The calculation of A is very similar, therefore we give only the final result for it. Similarly to the branch 1, the rescaled quantity $z = A/\bar{A}$ can be expressed as

$$z = \frac{A}{\bar{A}} = \frac{n+1}{n}(-a)^{-\frac{n+1}{n}}\left[\frac{2\sqrt{\pi}\,\Gamma(1+1/n)}{\Gamma(3/2+1/n)} - B_{-a}(1+1/n,1/2)\right], \qquad -1 < a < 0. \tag{81}$$

When a approaches its minimum value $a = -1$, z approaches z_c (given by equation (72)) above, therefore the branch 2 is valid for $z \geqslant z_c$. Substituting t_f and $A = z\,\bar{A}$ into equation (63), we obtain

$$S_{\mathrm{opt}} = \mathrm{Pe}\,\Phi_n^{(2)}\left(\frac{A}{\bar{A}}\right), \tag{82}$$

where $\Phi_n^{(2)}(z)$ is defined parametrically by the equation

$$\Phi_n^{(2)} = -1 + \frac{1}{n}(-a)^{-1/n}\left\{\frac{2\,\sqrt{\pi}\,\Gamma(1/n)}{\Gamma(1/2+1/n)} - B_{-a}[1/n,1/2]\right\} + \frac{a}{2(n+1)}\,z(a) \tag{83}$$

and equation (81). Although the solutions for the rate function $\Phi_n(z)$ for $z < z_c$ and $z > z_c$ come from two different branches, the function $\Phi_n(z)$ is analytic at $z = z_c$ for all $n > 0$.

The $z \to \infty$ asymptotic of $\Phi_n^{(2)}(z)$ is achieved in the limit of $a \to 0$, and we obtain

$$\Phi_n^{(2)}(z \to \infty) = \left(2^{-1/n}\,z_c\right)^{n/(n+1)}\,z^{1/(n+1)}\,. \tag{84}$$

Using this result in equation (73), we obtain from equation (55) the asymptotic result, presented in the second line of equation (8) in the Introduction.

For some values of n the special functions in equations (81) and (83) become elementary functions. A simple and instructive case is $n = 1$. Here equations (81) and (83) become

$$\begin{aligned} z &= \frac{(8-4a)\sqrt{a+1}+8}{3a^2}, \\ \Phi_1^{(2)} &= -\frac{(a+4)\sqrt{a+1}+3a+4}{3a}. \end{aligned} \tag{85}$$

Eliminating a, one can obtain the explicit rate function

$$\Phi_1(z) = \frac{2}{9z}\left[(1+3z)^{3/2} - 9z + 1\right], \tag{86}$$

which in fact holds for all $0 < z < \infty$. Figure 3 shows the plot of $\Phi_1(z)$.

J. Stat. Mech. (2020) 023202

3.2.2. $-1 < n < 0$. Dynamical phase transition. For $-1 < n < 0$ the OFM predicts a dramatic difference between the regimes of $A < \bar{A}$ and $A > \bar{A}$. Remarkably, for $A > \bar{A}$ the rate function $\Phi_n(z)$ is equal to zero. Indeed, to achieve an arbitrary large A, the particle can follow the zero-action *noiseless* path (59) almost until $t_f = x_0/\mu$. Arbitrarily close to t_f, when $x(t)$ is already very close to zero, we can change the path a little, and make the functional (3) arbitrary large. The resulting action can be made arbitrary small. For $A < \bar{A}$ the action is nonzero, and we will calculate it shortly. These calculations will show that the system exhibits a dynamical phase transition[6] at $A = \bar{A}$.

Let us determine the optimal path and the action for $A < \bar{A}$, and start with determining the energy E of the effective Newtonian particle. For $-1 < n < 0$, $x_n(t_f)$ diverges. Therefore, instead of equation (58), we will use a different argument. Let us express $\mathcal{A}$ in terms of E and λ. For $n < 0$ and $A < \bar{A}$, the optimal path $x(t)$ must be monotone decreasing, so the energy integral (57) yields equation (65). As a result,

$$\mathcal{A} = \int_0^{t_f} [x(t)]^n \, \mathrm{d}t = \int_0^{x_0} \frac{\mathrm{d}x \, x^n}{\sqrt{2(E + \lambda x^n)}}. \tag{87}$$

At $\lambda = 0$ the optimal path is noiseless, and equation (87) must give $\mathcal{A} = \bar{A}$, as in equation (60). This leads to $E = \mu^2/2$ as in the case of $n > 0$. Equation (63) remains valid here, and we need to express A and the optimal value of t_f through λ, D, μ and x_0. Since $A < \bar{A}$, λ must be positive (see equation (87)). Figure 4 shows the dependence of $A/\bar{A}$ on $a = \lambda/\lambda_c$, which is described by equation (90), in the particular case $n = -2/3$.

To reach $x = 0$ the particle must move toward $x = 0$ from the start, and we again arrive at equations (65) and (66), although for $n < 0$ the final expressions are different. Introducing $u = x/x_0$ and $a = 2\lambda x_0^n/\mu^2$, we obtain

$$t_f = \frac{x_0}{\mu} \left[{}_2F_1\left(\frac{1}{2}, \frac{1}{n}; 1 + \frac{1}{n}; -a\right) - \frac{a^{-1/n} \Gamma\left(\frac{1}{2} - \frac{1}{n}\right) \Gamma\left(1 + \frac{1}{n}\right)}{\sqrt{\pi}} \right]; \quad 0 \leqslant a < \infty, \quad -1 < n < 0. \tag{88}$$

Now we express A via a from equation (87) with $E = \mu^2/2$:

$$A = \int_0^{t_f} x^n(t) \, \mathrm{d}t = \int_0^{x_0} \frac{x^n \, \mathrm{d}x}{\sqrt{2\lambda x^n + \mu^2}}. \tag{89}$$

In terms of the dimensionless variable $z = A/\bar{A}$, equation (89) gives

$$z = \frac{A}{\bar{A}} = \frac{2(n+1)}{(n+2)\sqrt{a}} \, {}_2F_1\left(\frac{1}{2}, -\frac{n+2}{2n}; \frac{1}{2} - \frac{1}{n}; -\frac{1}{a}\right), \quad 0 < z < 1. \tag{90}$$

Plugging the expressions for t_f from equation (88) and $z = A/\bar{A}$ from equations (90) into (63), we can represent S_{opt} (and hence $-\ln P_n(A|x_0)$) in the scaling form

$$-\ln P_n(A|x_0) \simeq S_{\mathrm{opt}} = \mathrm{Pe} \, \Phi_{-1<n<0}\left(z = \frac{A}{\bar{A}}\right), \tag{91}$$

where the scaling function $\Phi_{-1<n<0}(z)$ is given in a parametric form by equation (90) and the equation

[6] A sharp transition occurs only in the limit of $\mathrm{Pe} \to \infty$. We expect that at finite but large Pe, the transition is smoothed on a narrow interval around $A = \bar{A}$, the width of which scales as a negative power of Pe.

J. Stat. Mech. (2020) 023202

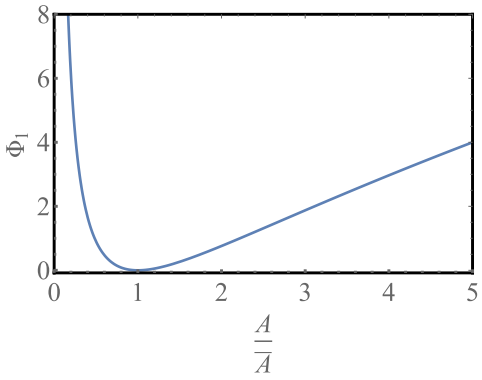

Figure 3. The rate function $\Phi_1(A/\bar{A})$, described by equation (86).

$$\Phi_{-1<n<0} = -1 - \frac{a^{-1/n}\Gamma\left(\frac{1}{2}-\frac{1}{n}\right)\Gamma\left(1+\frac{1}{n}\right)}{\sqrt{\pi}} +_2 F_1\left(\frac{1}{2},\frac{1}{n};1+\frac{1}{n};-a\right) + \frac{az(a)}{2(n+1)}\,, \tag{92}$$

where $0 \leqslant a < \infty$. Let us recall that, $z = A/\bar{A} \to 0$ corresponds to $a = 2\lambda x_0^n/\mu^2 \to \infty$, while $z \to 1$ from below implies $a \to 0$, as in figure 4. As A increases from 0 to $\bar{A}$, λ decreases monotonically from ∞ to 0 for all $-1 < n < 0$.

What happens at $A > \bar{A}$? We note that λ cannot be negative for $-1 < n < 0$: otherwise, the effective potential energy $-\lambda x^n$ would go to plus infinity at $x \to 0$, making the arrival of our finite-energy Newtonian particle at $x = 0$ impossible. Therefore, as A increases beyond $\bar{A}$, λ must stick to its value at $A = \bar{A}$, which is zero. Since $\lambda = 0$ corresponds to a noiseless classical path as in equation (59), we obtain $S_{\rm opt} = 0$, and the rate function vanishes identically, as we already argued above.

Thus summarizing, for any $-1 < n < 0$ at large $\mathrm{Pe} = \mu x_0/2D$, the distribution $P_n(A|x_0)$ exhibits the scaling form

$$-\ln P_n(A|x_0) \simeq \mathrm{Pe}\,\Phi_n\left(z = \frac{A}{\bar{A}}\right)\,, \tag{93}$$

with the rate function

$$\Phi_n(z) = \begin{cases} \Phi_n^-(z), & z \leqslant 1, \quad (94) \\ 0, & z \geqslant 1, \quad (95) \end{cases}$$

where $\Phi_n^-(z)$ is nontrivial and is given parametrically in equation (92). In the next section we will show that $\Phi_n^-(z)$ vanishes as $(1-z)^{\alpha_n}$ as $z \to 1$ from below, with an n-dependent exponent α_n. For $-1/2 < n < 0$, we will obtain $\alpha_n = 2$, while for $-1 < n < -1/2$ $\alpha_n = (1-z)^{1/(n+1)}$. The non-analytic behavior of $\Phi_n(z)$ at $z = 1$ implies a dynamical phase transition, as announced in the Introduction.

The asymptotic of $\Phi_{-1<n<0}(z)$ as $z \to 0$ (that is, $a \to \infty$) coincides with that given by the first line in equation (75).

As before, it is instructive to consider specific values of n for which the hypergeometric functions in equations (90) and (92) become elementary functions. An especially simple case if $n = -2/3$, when equations (90) and (92) yield $z(a) = \sqrt{1+a} - \sqrt{a}$ and

J. Stat. Mech. (2020) 023202

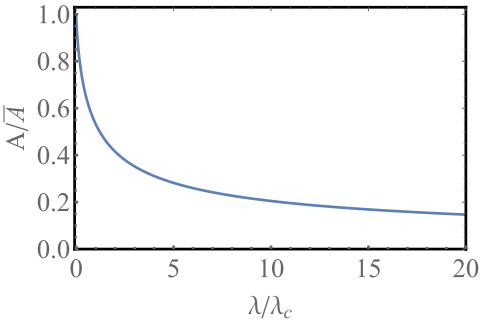

Figure 4. $z = A/\bar{A}$ versus $a = \lambda/\lambda_c$, where $\lambda_c = \mu^2/(2x_0^n)$, for $-1 < n < 0$ and $A < \bar{A}$ as described by equation (90). Here for any $\lambda > 0$ there is only one solution for the optimal path $x(t)$ and A. The specific example is $n = -2/3$, where $z = \sqrt{1+a} - \sqrt{a}$.

$\Phi_{-2/3}(a) = (1/2)\left[a^{3/2} + (2-a)\sqrt{1+a} - 2\right]$, respectively. Eliminating a and recalling that $\Phi_{-1<n<0} = 0$ for $z \geqslant 11$, we obtain an aesthetically beautiful elementary expression

$$\Phi_{-2/3}(z) = \begin{cases} \frac{(1-z)^3(z+3)}{8z}, & z \leqslant 1, \quad (96) \\ 0, & z \geqslant 1, \quad (97) \end{cases}$$

depicted in figure 5. It describes a dynamical phase transition of the third order at $z = 1$.

4. $\Phi_n(z)$ via WKB approximation

In this section we provide an alternative perturbative derivation of the rate function $\Phi_n(z)$ for all $n > -1$ in the large-Pe limit, starting from the exact differential equation (43). The method we use here is a variant of the dissipative WKB approximation [23]. We will see that it reproduces exactly the OFM result for all $n > -1$ in the large Pe-limit. Moreover, it provides a different representation of the rate function $\Phi_n(z)$ which is somewhat easier for the asymptotic analysis near $z = 1$ to determine the order of the dynamical phase transition at $z = 1$ for $-1 < n < 0$.

Our starting point is the exact differential equation (43) satisfied by the Laplace transform $Q_p(x_0)$. We start with the scaling ansatz (as anticipated from our OFM analysis in the previous section)

$$P_n(A) \sim \exp\left[-\frac{\mu x_0}{2D}\,\Phi_n\left(\frac{A}{\bar{A}}\right)\right], \qquad \bar{A} = \frac{x_0^{n+1}}{\mu\,(n+1)}, \quad (98)$$

in the Laplace transform $Q_p(x_0) = \int_0^\infty \mathrm{e}^{-p\,A}\,P_n(A)\,\mathrm{d}A$. We obtain, up to pre-exponential factors,

J. Stat. Mech. (2020) 023202

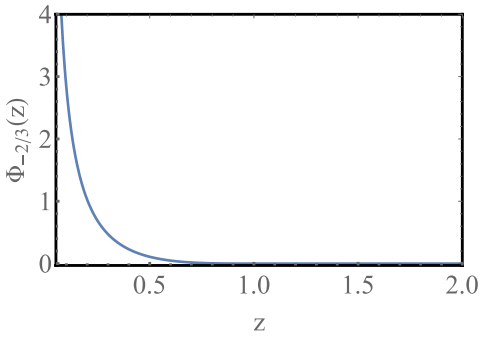

Figure 5. The rate function $\Phi_{-2/3}(z)$, as in equations (96) and (97), for the Brownian functional $\mathcal{A} = \int_0^{t_f} [x(t)]^{-2/3} \mathrm{d}t$. This system exhibits a dynamical phase transition of third order.

$$Q_p(x_0) \sim \int_0^\infty \mathrm{d}A \, \exp\left[-p\,A - \frac{\mu x_0}{2D}\,\Phi_n\left(\frac{A}{\bar{A}}\right)\right] \\ \sim \int_0^\infty \mathrm{d}z \, \exp\left\{-\frac{\mu x_0}{2D}\,\left[\Phi_n(z) + c\,p\,x_0^n\,z\right]\right\}, \qquad c = \frac{2\,D}{\mu^2\,(n+1)}\,. \tag{99}$$

When the Péclet number $\mathrm{Pe} = \mu x_0/2D$ is large, we can evaluate the integral in equation (99) by the saddle point method, while keeping the product $u = c\,p\,x_0^n$ fixed. This gives us the scaling ansatz in the Laplace space, for any $n > -1$:

$$Q_p(x_0) \sim \exp\left[-\frac{\mu x_0}{2D}\,\Psi_n(u = c\,p\,x_0^n)\right], \tag{100}$$

where the scaling function $\Psi_n(u)$ is given by the Legendre transform

$$\Psi_n(u) = \min_z \left[u\,z + \Phi_n(z)\right]. \tag{101}$$

Conversely, once $\Psi_n(u)$ is known, we can extract $\Phi_n(z)$ via the inverse Legendre transform

$$\Phi_n(z) = \max_u \left[-u\,z + \Psi_n(u)\right]. \tag{102}$$

Our immediate task, therefore, is to determine $\Psi_n(u)$ from equation (43) for $Q_p(x_0)$. Seeking the solution in the eikonal form

$$Q_p(x_0) = \mathrm{e}^{-s_p(x_0)/2D}, \tag{103}$$

we obtain an exact equation for $s_p(x_0)$:

$$-\frac{1}{2}Ds_p''(x_0) + \frac{1}{4}[s_p'(x_0)]^2 + \frac{\mu}{2}s_p'(x_0) - Dpx_0^n = 0. \tag{104}$$

The WKB approximation is again based on the large parameter $\mathrm{Pe} \to \infty$. In the leading WKB order [23] we can neglect the second-derivative term in equation (104) and express $s_p'(x_0)$ via x_0 from the ensuing quadratic equation for $s_p'(x_0)$[7]:

$$s_p'(x_0) = -\mu + \sqrt{\mu^2 + 4Dpx_0^n}. \tag{105}$$

J. Stat. Mech. (2020) 023202

Integrating this first-order equation, we obtain

$$s_p(x_0) = -\mu x_0 + \int_0^{x_0} \sqrt{\mu^2 + 4Dpx_0^n}\, \mathrm{d}x. \tag{106}$$

Comparing equations (100) and (103), we obtain $\Psi_n(u) = s_p(x_0)/(\mu x_0)$, where x_0 should be expressed through $u = c\,p\,x_0^n$. As in the OFM, the calculations in the cases $n > 0$ and $-1 < n < 0$ are slightly different, and we perform them separately[8].

4.1. $n \geqslant 0$

Here equation (106) yields, after rescalings,

$$\Psi_n(u) = -1 + \frac{1}{n\,u^{1/n}} \int_0^u \sqrt{1 + 2\,(n+1)\,v}\; v^{\frac{1}{n}-1}\, \mathrm{d}v = -1 + {}_2F_1\left[-1/2, 1/n, 1+1/n, -2\,(n+1)\,u\right]. \tag{107}$$

As a result, the rate function $\Phi_n(z)$ is given by

$$\Phi_n(z) = \max_u \left\{-u\,z - 1 + {}_2F_1\left[-1/2, 1/n, 1+1/n, -2\,(n+1)\,u\right]\right\}, \quad n \geqslant 0. \tag{108}$$

This expression is more compact than, but equivalent to, equation (74) that we obtained by the OFM. The two branches, which played a prominent role in section 3.2, appear here in the form of two different zeros of the u-derivative of the function inside the curly brackets in equation (108). Finally, we included $n = 0$ in the applicability domain of equation (108) because

$$\lim_{n\to 0} \Psi_0(u) = -1 + \sqrt{1 + 2\,u}, \tag{109}$$

and, as one can check,

$$\Phi_0(z) = \max_u \left(-u\,z - 1 + \sqrt{1 + 2\,u}\right) = \frac{(z-1)^2}{2z}, \tag{110}$$

which coincides with the large deviation function in the exponent of the exact expression (45) for $P_0(t_f|x_0)$.

4.2. $-1 < n < 0$. Dynamical phase transtion

In this case equation (106) yields

$$\begin{aligned}\Psi_n(u) &= -1 - \frac{1}{n\,u^{1/n}} \int_u^{\infty} \sqrt{1 + 2\,(n+1)\,v}\; v^{\frac{1}{n}-1}\, \mathrm{d}v \\ &= -1 + \frac{\sqrt{8(n+1)u}\,{}_2F_1\left[-\frac{1}{2}, -\frac{1}{2} - \frac{1}{n}; \frac{1}{2} - \frac{1}{n}; -\frac{1}{2(n+1)u}\right]}{n+2},\end{aligned} \tag{111}$$

[7] When solving the quadratic equation, we should discard the solution with the minus sign, to avoid a divergence of $Q_p(x_0)$ at $x_0 \to \infty$.

[8] For $n = 0$ the WKB result for $Q_p(x_0)$, described by equations (103) and (106), is exact and coincides with equation (44). Here $s_p(x_0)$ is proportional to x_0, and the neglected term with $s_p''(x_0)$ in equation (104) vanishes identically.

J. Stat. Mech. (2020) 023202

and the rate function is

$$\Phi_n(z) = \max_u \left\{ -u\,z - 1 + \frac{\sqrt{8(n+1)u}\,{}_2F_1\left[-\frac{1}{2}, -\frac{1}{2} - \frac{1}{n}; \frac{1}{2} - \frac{1}{n}; -\frac{1}{2(n+1)u}\right]}{n+2} \right\}, \quad -1 < n < 0. \tag{112}$$

As $u \to 0$, the leading-order asymptotic of $\Psi_n(u)$ is u. The corresponding leading-order asymptotic of the function $-uz + \Psi_n(u)$ is $(1-z)u$; it is positive for $z < 1$ and negative for $z > 1$. As a result, the function $-uz + \Psi_n(u)$ has a local maximum at some $u = u(z) > 0$ only when $z < 1$. For $z \geqslant 1$ the maximum is always achieved at $u = 0$, and the maximum value is zero. Therefore, in full agreement with the OFM results of section 3.2.2, the rate function $\Phi_n(z)$, as described by equation (112), is nonzero at $z < 1$ and zero for all $z \geqslant 1$:

$$\Phi_n(z) = \begin{cases} \Phi_n^-(z), & z \leqslant 1, \qquad (113) \\ 0, & z \geqslant 1, \qquad (114) \end{cases}$$

where the function $\Phi_n^-(z)$ is given in equation (112). One can show that equation (112) and the OFM result, described by equations (90) and (92), are exactly equivalent.

Order of the dynamical phase transition. To determine the order of the dynamical phase transition at $z = 1$, we should extract the leading-order asymptotic of $\Phi_n(z)$ at $1 - z \ll 1$. This asymptotic corresponds to the $u \to 0$ asymptotic of the function $\Psi_n(u)$ from equation (111) which includes the leading linear term and the first subleading nonlinear term. The latter asymptotic depends on whether $1/2 < n < 0$ or $-1 < n < -1/2$:

$$\Psi_n(u \to 0) = \begin{cases} u - \frac{(n+1)^2}{2(2n+1)}\,u^2 + \ldots, & -\frac{1}{2} < n < 0, \qquad (115) \\ u - C_n\,u^{-\frac{1}{n}} + \ldots, & -1 < n < -\frac{1}{2}, \qquad (116) \end{cases}$$

where

$$C_n = -\frac{\Gamma\left(1 + \frac{1}{n}\right)\Gamma\left(-\frac{1}{2} - \frac{1}{n}\right)}{2^{1+\frac{1}{n}}\sqrt{\pi}(n+1)^{\frac{1}{n}}} > 0. \tag{117}$$

In the marginal case $n = -1/2$ we obtain a quadratic subeading term with a logarithmic correction:

$$\Psi_{-1/2}(u \to 0) = u - \frac{1}{4}\,u^2\,\ln\left(\frac{1}{u}\right) + \ldots. \tag{118}$$

At $-1/2 < n < 0$ we use equations (112) and (115) to obtain

$$\Phi_n^-(z) \simeq \frac{(2n+1)}{2(n+1)^2}\,(1-z)^2, \quad 1 - z \ll 1. \tag{119}$$

This expression describes small one-sided Gaussian fluctuations of $A < \bar{A}$. For all $-1/2 < n < -0$, the rate function $\Phi_n(z)$ is continuous together with its first derivative at $z = 1$. The second derivative has a discontinuity, so the dynamical phase transition in this case is of second order.

J. Stat. Mech. (2020) 023202

For $-1 < n < -1/2$, we use equations (112) and (116) to obtain, close to $z = 1$,

$$\Phi_n^-(1-z \ll 1) \simeq \frac{1}{2}\pi^{-\frac{n}{2n+2}} \left[\Gamma\left(2+\frac{1}{n}\right)\Gamma\left(-\frac{1}{2}-\frac{1}{n}\right)\right]^{\frac{n}{n+1}} (1-z)^{\frac{1}{n+1}}. \quad (120)$$

In this regime small fluctuations of A around the mean value $\bar{A}$ are non-Gaussian. Furthermore, the order of the phase transition at $z = 1$ now continuously depends on n. As n varies from $-1/2$ to -1, the order of transition continuously increases from 2 to infinity. In general, it is non-integer and not even rational. This intricate behavior is quite remarkable.

In the marginal case $n = -1/2$ we use equations (112) and (118) to obtain, to leading order

$$\Phi_{-1/2}^-(1-z \ll 1) \simeq \frac{(1-z)^2}{\ln\left(\frac{1}{1-z}\right)}. \quad (121)$$

Finally, using the $u \to \infty$ asymptotic of equation (111),

$$\Psi_n(u \to \infty) \simeq \frac{2\sqrt{2(n+1)u}}{n+2}, \quad (122)$$

and equation (112), we checked that, to leading order, the $A \to 0$ asymptotic of $-\ln P_n(A, x_0)$ is equal to $\nu^2 x_0^{1/\nu}/(DA)$, in agreement with the exact result (5) obtained for $\mu = 0$.

In the particular case $n = -2/3$ the calculations simplify dramatically. Here we obtain

$$\Psi_{-2/3}(u) = \frac{1}{9}\left(2u\sqrt{6u+9} - 2\sqrt{6}\,u^{3/2} + 3\sqrt{6u+9} - 9\right), \quad (123)$$

and the maximization in equation (112) yields equations (96) and (97) of section 3.2.2.

5. Discussion

In the first part of the paper, we studied the distribution of the functional $\mathcal{A} = \int_0^{t_f} x^n(t)\,\mathrm{d}t$, where $x(t)$ represents a Brownian motion with diffusion constant D, starting at $x_0 > 0$, and t_f represents the time of the first-passage to the origin. We computed the PDF $P_n(A|x_0) = \text{Prob.}(\mathcal{A} = A)$ exactly for all $n > -2$, when this PDF is well defined. The PDF exhibits an essentially singularity as $A \to 0$ and a fat tail $\sim A^{-(n+3)/(n+2)}$ as $A \to \infty$. We complemented our exact analysis by employing the OFM. In OFM, one seeks the optimal path that minimizes the effective classical action. The latter yields (the minus logarithm of) the PDF in the leading order. As we showed, the OFM correctly reproduces the leading essential singular tail at $A \to 0$. The OFM, however, cannot be used for a description of the fat tail for large A. This is because the power-law behavior for large A arises from the contributions of many competing stochastic trajectories, and there is not one single optimal path that would dominate this tail. An added value of the OFM analysis, when it applies, is a detailed prediction of the optimal path

J. Stat. Mech. (2020) 023202

that is not readily available in the exact method. The optimal path gives an instructive visual insight into the nature of large deviations in the system. It would be interesting to observe the optimal path in experiments/numerical simulations.

In the second part of the paper we studied the PDF $P_n(A|x_0)$ of the same functional as above, but now $x(t)$ is a Brownian motion with a nonzero drift μ. In this case the PDF is well defined only for $n > -1$.

For a drift toward the origin ($\mu > 0$), an explicit result for the PDF $P_n(A|x_0)$ is available only for $n = 0$. It is here where the OFM becomes an invaluable tool, and not just a complementary technique: it allows to determine the tails of $P_n(A|x_0)$ for any $n > -1$. The OFM results can be understood in terms of the dimensionless Péclet number $\mathrm{Pe} = \mu x_0/(2D)$ that shows the relative role of the drift and diffusion. There are two important aspects of the OFM results for $P_n(A|x_0)$:

- For arbitrary Pe, OFM correctly predicts both tails of $P_n(A|x_0)$: $A \to 0$ and $A \to \infty$. In the former case one again finds essential singular behavior as in the driftless case. In the latter case $P_n(A|x_0)$ has a stretched exponential tail, $-\ln P_n(A|x_0) \sim A^{-1/(n+1)}$ for $n > 0$.
- For large Pe, OFM captures the exact PDF $P_n(A|x_0)$ *for all* A. In this case we showed that $-\ln P_n(A|x_0) \simeq \mathrm{Pe}\,\Phi_n\left(z = A/\bar{A}\right)$ with $\bar{A} = x_0^{n+1}/\mu(n+1)$. We computed the rate function $\Phi_n(z)$ analytically.

We have also shown that the OFM results can be reproduced by an alternative asymptotic perturbative theory—the dissipative WKB approximation. While the OFM can be viewed as a WKB approximation in the 'real space', the second method is analogous, due to a Legendre transformation involved, to a WKB approximation in the 'momentum space'.

One interesting conclusion of our large-Pe analysis is that, for $-1 < n < 0$, the function $\Phi_n(z)$ is non-analytic at $z = 1$ thus describing a dynamical phase transition. Remarkably, the order of this transition depends on n—while it is second order for $-1/2 < n < 0$, the order is $1/(n+1)$ for $-1 < n < -1/2$. A sharp transition, however, occurs only in the limit of $\mathrm{Pe} \to \infty$. We expect that at finite but large Pe, the transition is smoothed on a narrow interval around $A = \bar{A}$, the width of which scales as a negative power of Pe.

We remark that the mechanism behind the dynamical phase transition with varying order of the transition at $-1 < n < -1/2$ is very different from the mechanism of similarly looking singularities in the rate function describing the free energy in a class of multicritical matrix models [24–29] (see also [30] and [31] for slightly different perspectives based on extreme statistics in matrix models). In the latter case the order of the phase transition near the so-called double scaling limit can also be varied by varying the degree of the polynomial describing the matrix potential. In our case, however, the transition occurs in a much simpler setting of a single particle.

Finally, we employed the OFM to study the case of $\mu < 0$ (drift away from the origin), see the appendix. We showed that, when the process is conditioned on reaching the origin, the distribution of $\mathcal{A}$ coincides, in the limit of large Pe, with the distribution of $\mathcal{A}$ for $\mu > 0$ with the same value of $|\mu|$. In the case of $n = 0$ this duality between the

J. Stat. Mech. (2020) 023202

two settings is known to be exact, that is to hold for any Pe [32]. It would be interesting to see whether it is also exact for $n \neq 0$.

Acknowledgments

BM was supported by the Israel Science Foundation (Grant No. 807/16) and by a Chateaubriand fellowship of the French Embassy in Israel. He is very grateful to the LPTMC, Sorbonne Université, for hospitality.

Appendix. Outward drift

For outward drift, $\mu < 0$, the probability that the particle ultimately reaches $x = 0$, is [3]

$$P_0 = \mathrm{e}^{-\frac{|\mu| x_0}{D}} \equiv \mathrm{e}^{-2\mathrm{Pe}}. \tag{A.1}$$

Suppose that the Péclet number

$$\mathrm{Pe} = \frac{|\mu| x_0}{2D} \tag{A.2}$$

is much larger than 1. Then the probability (A.1) of ever reaching zero is exponentially small. Still, one can ask a similar question about the probability density of the Brownian functional $\mathcal{A}$ from equation (3) when the process is conditioned on reaching $x = 0$. Within the framework of the OFM, this conditional probability density is equal to the ratio of the probability densities of two different optimal paths: with and without the constraint $\mathcal{A} = A$. Equivalently, the optimal constrained action is equal to the difference of the actions of the optimal paths with and without the constraint. For completeness, we first show, within the framework of the OFM, that the unconstrained action is equal to 2Pe in agreement with the exact result (A.1). In the absence of constraint on $\mathcal{A}$, the Euler–Lagrange equation (56) becomes simply $\ddot{x} = 0$. Its solutions, obeying the initial condition $x(0) = x_0$ and the condition of reaching $x = 0$ at some time t_f, can be written as $x(t) = x_0(1 - t/t_f)$. The unconstrained action is, therefore,

$$S = \frac{1}{4D}\int_0^{t_f} (\dot{x} + \mu)^2 \, \mathrm{d}t = \frac{1}{4D}\int_0^{t_f} \left(-\frac{x_0}{t_f} + \mu\right)^2 \mathrm{d}t = \frac{1}{4D}\left(\frac{x_0^2}{t_f} + \mu^2 t_f - 2\mu x_0\right). \tag{A.3}$$

Now we should minimize this expression with respect to the first-passage time t_f. The minimum value of S is achieved at $t_f = x_0/|\mu|$: the optimal unconstrained path describes ballistic motion with the velocity equal to the *minus* deterministic drift velocity. The resulting optimal unconstrained action, as obtained from equation (A.3), is equal to $|\mu| x_0/D = 2\mathrm{Pe}$, as to be expected from equation (A.1). Notice that the corresponding optimal unconstrained value of $\mathcal{A}$,

$$A_0 = \frac{x_0^{n+1}}{|\mu|(n+1)}, \tag{A.4}$$

coincides, up to the change $\mu \to |\mu|$, with $\bar{A}$ from equation (11).

J. Stat. Mech. (2020) 023202

Now we should find the optimal path constrained by $\mathcal{A} = A$. The Euler–Lagrange equation (56), the initial condition $x(0) = x_0$ and the constraint $\mathcal{A} = A$ do not depend on μ. The μ-dependence comes only from the value of the energy E of the effective Newtonian particle in equation (57). As one can show, it is equal to $E = \mu^2/2$ as before[9]. The offshoot is that, for a fixed λ, the optimal path for $\mu < 0$ *coincides* with the optimal path for $\mu > 0$ with the same $|\mu|$. As a result, A as a function of the Lagrange multiplier λ in the two problems with the same $|\mu|$ is exactly the same.

The optimal actions in these two problems, S_μ and $S_{-\mu}$ (where $\mu < 0$), are of course different. Let us evaluate their difference. We have

$$S_\mu - S_{-\mu} = \frac{1}{4D}\int_0^{t_f} (\dot{x}+\mu)^2\,\mathrm{d}t - \frac{1}{4D}\int_0^{t_f} (\dot{x}-\mu)^2\,\mathrm{d}t = \frac{1}{4D}\int_0^{t_f} 2\mu \times 2\dot{x}\,\mathrm{d}t = \frac{|\mu|x_0}{D} = 2\mathrm{Pe}, \quad \mu < 0. \tag{A.5}$$

Therefore, $S_\mu = S_{-\mu} + 2\mathrm{Pe}$. After subtracting the unconditioned action—which is also equal to 2Pe—we arrive at

$$-\ln P_n^{(\mu<0)}(A) \simeq S_{-\mu} = \mathrm{Pe}\,\Phi_n\left(\frac{A}{A_0}\right), \tag{A.6}$$

where Pe is defined in equation (A.2), and $\Phi_n(z)$ was calculated in section 3.2.1 for $n > 0$, and in section 3.2.2 for $-1 < n \leqslant 0$. That is, all our results for the rate function in the case of favorable drift (the asymptotics, the dynamical phase transition at $-1 < n < 0$, etc) also hold for the unfavorable drift with the same value of $|\mu|$, if the latter process is conditioned on reaching $x = 0$. In the particular case $n = 0$ this duality has been previously established (exactly, that is for any value of Pe) in [32].

References

[1] Majumdar S N 2005 Brownian functionals in physics and computer science *Curr. Sci.* **89** 2076
[2] Kac M 1949 On distributions of certain wiener functionals *Trans. Am. Math. Soc.* **65** 1
[3] Redner S 2001 *A Guide to First-Passage Processes* (Cambridge: Cambridge University Press)
[4] Bray A J, Majumdar S N and Schehr G 2013 Persistence and first-passage properties in nonequilibrium systems *Adv. Phys.* **62** 225
[5] Kearney M J and Majumdar S N 2005 On the area under a continuous time Brownian motion till its first-passage time *J. Phys. A: Math. Gen.* **38** 4097
[6] Dhar D and Ramaswamy R 1989 Exactly solved model of self-organized critical phenomena *Phys. Rev. Lett.* **63** 1659
[7] Kearney M J 2004 On a random area variable arising in discrete-time queues and compact directed percolation *J. Phys. A: Math. Gen.* **37** 8421
[8] Prellberg T and Brak R 1995 Critical exponents from nonlinear functional equations for partially directed cluster models *J. Stat. Phys.* **78** 701
[9] Richard C 2002 Scaling behavior of two-dimensional polygon models *J. Stat. Phys.* **108** 459
[10] Majumdar S N and Kearney M J 2007 On the inelastic collapse of a ball bouncing on a randomly vibrating platform *Phys. Rev.* E **76** 031130
[11] Hammersley J M 1961 On the statistical loss of long period comets from the solar system II *Proc. 4th Berkeley Symp. on Mathematical Statistics and Probability* vol 3 (Berkeley, CA: University of California Press) pp 17–78

[9] One way to show it, valid for all $n > -1$, is to use the fact that at $\lambda = 0$ one obtains the unconstrained optimal path, for which one has $A = A_0$ as in equation (A.4)

J. Stat. Mech. (2020) 023202

[12] Dean D S and Majumdar S N 2001 The exact distribution of the oscillation period in the underdamped one-dimensional Sinai model *J. Phys. A: Math. Gen.* **34** L697
[13] Grosberg A and Frisch H 2003 Winding angle distribution for planar random walk, polymer ring entangled with an obstacle, and all that: Spitzer–Edwards–Prager–Frisch model revisited *J. Phys. A: Math. Gen.* **36** 8955
[14] Meerson B 2019 Large fluctuations of the area under a constrained Brownian excursion *J. Stat. Mech.* 013210
[15] Smith N R and Meerson B 2019 Geometrical optics of constrained Brownian excursion: from the KPZ scaling to dynamical phase transitions *J. Stat. Mech.* 023205
[16] Meerson B and Smith N R 2019 Geometrical optics of constrained Brownian motion: three short stories *J. Phys. A: Math. Theor.* **52** 415001
[17] Agranov T, Zilber P, Smith N R, Admon T, Roichman Y and Meerson B 2019 The Airy distribution: experiment, large deviations and additional statistics (arXiv:1908.08354)
[18] Kearney M J, Majumdar S N and Martin R J 2007 The first-passage area for drifted Brownian motion and the moments of the Airy distribution *J. Phys. A: Math. Theor.* **40** F863
[19] Kearney M J and Majumdar S N 2014 Statistics of the first passage time of Brownian motion conditioned by maximum value or area *J. Phys. A: Math. Theor.* **47** 465001
[20] Majumdar S N and Comtet A 2002 Exact asymptotic results for persistence in the Sinai model with arbitrary drift *Phys. Rev.* E **66** 061105
[21] Abramowitz M and Stegun I A 1973 *Handbook of Mathematical Functions* (New York: Dover)
[22] Gradshteyn I S and Ryzhik I M 1980 *Tables of Integrals, Series and Products* 5th edn (London: Academic)
[23] Bender C M and Orszag S A 1999 *Advanced Mathematical Methods for Scientists and Engineers I: Asymptotic Methods and Perturbation Theory* (New York: Springer)
[24] Gross D J and Witten E 1980 Possible third-order phase transition in the large-N lattice gauge theory *Phys. Rev.* D **21** 446
[25] Wadia S R 1980 $N = \infty$ phase transition in a class of exactly soluble model lattice gauge theories *Phys. Lett.* B **93** 403
[26] Brézin E 1992 *Matrix Models of Two Dimensional Quantum Gravity* (*Les Houches lecture notes*) ed B Julia and J Zinn Justin (Amsterdam: North-Holland)
[27] Douglas M R and Kazakov V A 1993 Large N phase transition in continuum QCD2 *Phys. Lett.* B **319** 219
[28] Gross D J and Matytsin A 1994 Instanton induced large N phase transitions in two- and four-dimensional QCD *Nucl. Phys.* B **429** 50
[29] Marino M 2006 *Matrix Models and Topological Strings* (*Applications of Random Matrices in Physics*) (Berlin: Springer) pp 319–78
[30] Majumdar S N and Schehr G 2014 Top eigenvalue of a random matrix: large deviations and third order phase transition *J. Stat. Mech.* P01012
[31] Le Doussal P, Majumdar S N and Schehr G 2018 Multicritical edge statistics for the momenta of fermions in nonharmonic traps *Phys. Rev. Lett.* **121** 030603
[32] Krapivsky P L and Redner S 2018 First-passage duality *J. Stat. Mech.* 093208

J. Stat. Mech. (2020) 023202